Chemical Engineering Journal 83 (2001) 215–217

Chemical Engineering Journal

www.elsevier.com/locate/cej

Short communication

Velocity profiles of air impinging on a two-dimensional confined rigid surface

D. Khummongkol*, T. Saonam, W. Netrbungon, O. Ngearnthaworn

Chemical and Process Engineering Program, Department of Chemical and Environmental Engineering, College of Engineering and Technology, Rangsit University, Patumtani 12000, Thailand

Received 3 April 2000; received in revised form 2 October 2000; accepted 4 October 2000

Abstract

We measured the velocity (v_y) of air impinging on a two-dimensional confined rigid surface for various nozzle sizes (D_n), nozzle heights from the floor (H_n) and nozzle air velocities (v_n). With the measured data, we obtained an empirical relationship to predict v_y: $v_y/v_n = (0.09 - 1.09\,e^{-12x/W})(y/H_n)^{0.13}$, where W is the impinger half-width.

Keywords: Velocity; Two-dimensional; Rigid surface; Impinger

1. Introduction

Impingement of gas on the surface of a water column was recently investigated as a means to remove tar and particulates from gas produced from biomass gasification [1–6]. The method was found to have removal efficiencies higher than 85% for tar [1] and about 80% for particulates with sizes smaller than 7.8 μm [2,3]. Moreover, the hot gas was cooled, hence increasing in the energy per volume [1,4]. Assuming that the air jet impinged on the floor of a cylinder was potential-flow [5,6], a removal efficiency was predicted to be less than 10% for 62 μm dust [5], a value much lower than the experimental value [3]. We believed that the removal efficiency may be predicted more accurately if the velocity profile of the gas was obtained. It is thus the objective of this study to monitor the velocity profile of air impinging on the floor of a two-dimensional impinger.

2. Experimental procedure

Fig. 1 is a schematic of the apparatus. Air from a 1 hp blower was passed through an 1 in. PVC pipe. Its velocity was regulated by a valve and measured by using a calibrated orifice meter. The impinger was rectangular and made of acrylic and its top was open for the air to leave the system. Its dimensions were 5 cm deep, 50 cm wide and 100 cm high. The nozzle was situated at the center of the rectangle. Three sizes of the nozzle (1.27, 1.91 and 2.54 cm diameter) and two heights of the nozzle from the impinger floor (5 and 15 cm) were used in this study. Due to symmetry, 1 cm holes were punched on one half of the impinger side, the holes were 0.5 cm apart as illustrated in Fig. 2. All the holes were covered with paper tape and one of them was open only when the air velocities in x- and y-directions at that position were measured by an Alnor Meter System 1, Model 360. The air velocity at the nozzle exit was set at 5 and 10 m/s, respectively.

3. Results and discussion

For our system, the method of dimensional analysis renders

$$\frac{v_y}{v_n} = f\left(\frac{x}{W}, \frac{y}{H_n}, \frac{D_n}{W}\right), \quad (1)$$

where W is the column half-width, v_y the air velocity in y-direction, v_n the air velocity at the nozzle exit, D_n and H_n are the nozzle diameter and the nozzle height from the floor, respectively. The ratio v_y/v_n is the reduced y-velocity.

Fig. 3 illustrates the effect of the nozzle diameter on the velocity profile at $y = 1.5$ and 7.5 cm from the floor.

* Corresponding author. Tel.: +662-997-2222; fax: +662-533-9470.
E-mail address: damrong@rangsit.rsu.ac.th (D. Khummongkol).

1385-8947/01/$ – see front matter
PII: S1385-8947(00)00279-5

Nomenclature

a, *b*, *c*, *d*	constants in Eq. (3)
D_n	nozzle diameter
H_n	nozzle height from floor
v_n	velocity at the nozzle exit
v_y	velocity in *y*-direction
W	impinger half-width

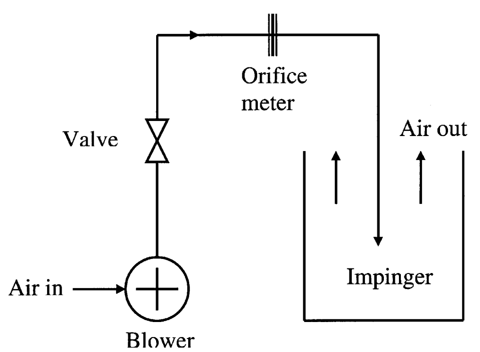

Fig. 1. Schematic of the apparatus.

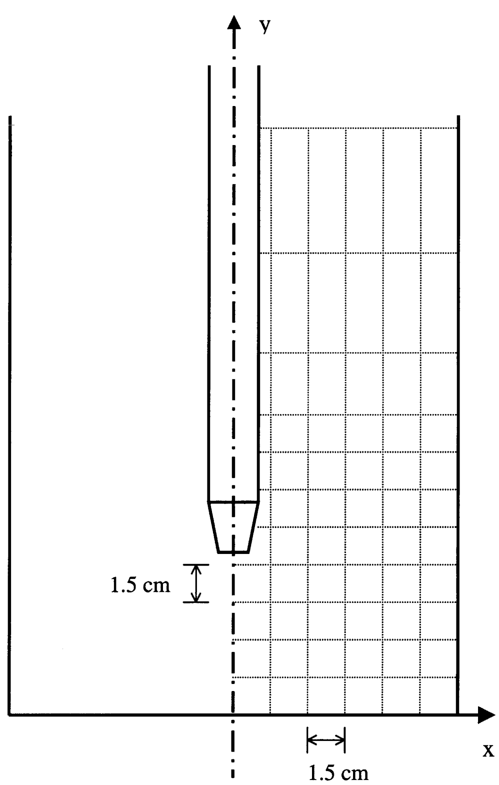

Fig. 2. Schematic of the impinger (intersections of the dotted lines are 1 cm holes).

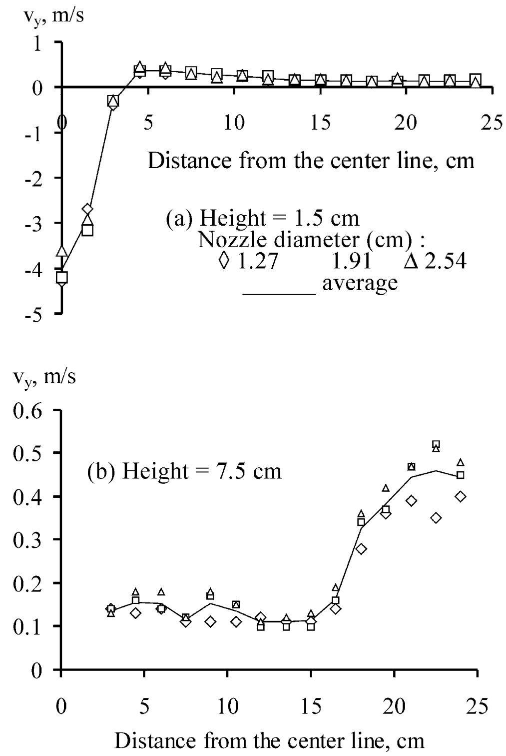

Fig. 3. Effect of the nozzle diameter on the profile of the *y*-velocity when $H_n = 5$ cm, $v_n = 5$ m/s.

Interestingly, the velocity profiles from different nozzle diameters in the regions below and above the nozzle almost coincided. Similar results were observed for the nozzle height of 15 cm. It implies that the *y*-velocity within the study conditions did not depend on the nozzle diameter. With the independence of D_n, Eq. (1) becomes

$$\frac{v_y}{v_n} = f\left(\frac{x}{W}, \frac{y}{H_n}\right). \tag{2}$$

Fig. 4 illustrates the relationship between the experimental reduced *y*-velocity and *x*/*W* for different values of y/H_n. There were 612 experimental values. At $x/W = 0$, v_y/v_n

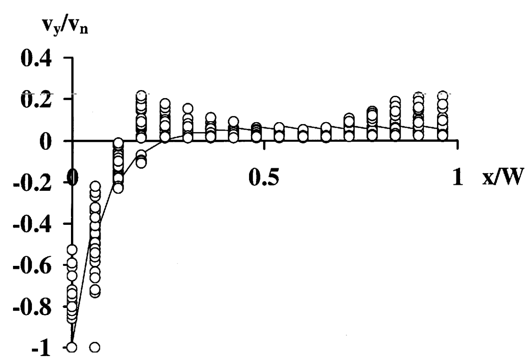

Fig. 4. Estimated velocity profile of v_y in the region under the nozzle: (○) experimental values; (- - - -) value estimated by Eq. (6).

varied from −1 to −0.5 due to different values of y/H_n. Similar results were observed at other values of x/W.

3.1. Empirical relationship of reduced y-velocity

From the velocity profile in the region under the nozzle in Fig. 4, we suggest the relationship of Eq. (2) in the following form:

$$\frac{v_y}{v_n} = \{a + b\,\mathrm{e}^{-cx/W}\}\left(\frac{y}{H_n}\right)^d, \tag{3}$$

where a, b, c and d are constants.

At the nozzle exit where $x = 0$ and $y/H_n = 1$, $v_y/v_n = -1$. Thus, Eq. (3) yields

$$a + b = -1. \tag{4}$$

Moreover, a mass balance across any cross-section gives

$$\int_0^W v_y\,\mathrm{d}x = 0. \tag{5}$$

We will use the above equations to fit the experimental data. By using the steepest gradient method [7] to minimize the sum of squares of the error, we obtain

$$\frac{v_y}{v_n} = (0.09 - 1.09\,\mathrm{e}^{-12x/W})\left(\frac{y}{H_n}\right)^{0.13}. \tag{6}$$

The reduced y-velocity predicted by the above equation is shown as a solid line on Fig. 4. The prediction had the same trend as the experimental values. The average absolute error was about 120% with the standard deviation of 150%. Most of the deviation occurred in the ranges of x/W between 0.1 and 0.3 and x/W greater than 0.7. It should be noted that at a particular value of x/W, more than one value of v_y/v_n was predicted due to y/H_n. Consequently, the predicted line appears discontinuous in the figure.

4. Conclusions

We developed a simple empirical relationship that may be used to predict the velocity profile of an air jet impinging on a confined surface.

References

[1] D. Khummongkol, C. Tangsathitkulchai, A model for tar-removal efficiency from biomass-produced gas impinging on a water surface, Energy 14 (1989) 113–121.

[2] D. Khummongkol, P. Khummongkol, in: Proceedings of the Fourth APCChE Congress, Singapore, May 13–15, 1987.

[3] D. Khummongkol, B. Saniam, V. Phimolmas, Removal of dust by impingement of gas on a water surface, Energy 17 (1992) 1007–1011.

[4] D. Khummongkol, P. Khummongkol, Heat transfer between an impinging air jet and an impinged water surface, Energy 23 (1998) 239–245.

[5] D. Khummongkol, P. Khummongkol, Theoretical analysis of dust removal from gas impinging on a confined liquid surface, Energy 19 (1994) 817–824.

[6] D. Khummongkol, P. Khummongkol, Finite-element analysis of air impinging on a confined liquid surface, RSU JET 2 (2) (1998) 20–22.

[7] T.F. Edgar, D.M. Himmelblau, Optimization of Chemical Processes, McGraw-Hill, New York, 1989.